JOURNAL OF CATALYSIS 135, 1–12 (1992)

MoO_3/MgO Systems: Effect of Preparation Method on Their Physicochemical Properties

JOSÉ M. M. LLORENTE,*,[1] VICENTE RIVES,*,[2] PILAR MALET,† AND FRANCISCO J. GIL-LLAMBÍAS‡

*Departamento de Química Inorgánica, Universidad de Salamanca, Facultad de Farmacia, 37007-Salamanca, Spain; †Departamento de Química Inorgánica, Universidad de Sevilla, Facultad de Química, 41012-Sevilla, Spain; and ‡Departamento de Química, Facultad de Ciencia, Universidad de Santiago de Chile, Chile

Received January 2, 1991; revised August 16, 1991

MoO_3/MgO systems have been prepared and characterized by X-ray diffraction, specific surface area and porosity measurements, visible–ultraviolet (diffuse reflectance) and Fourier transform infrared spectroscopies, differential thermal analysis, determination of the surface isoelectric point, and temperature-programmed reduction to analyze how the preparation method and pretreatments regulate their surface properties. Formation of $MgMoO_4$ on the surface of the support under certain experimental conditions stabilizes the surface of the support, thus avoiding its sintering during calcination at high temperature; in addition, reduction of Mo(VI) species in this case is more difficult, taking place at temperatures higher than those for bulk or supported molybdena.

INTRODUCTION

It has often been mentioned that the type of material used as a support for a heterogeneous catalyst, in addition to playing the expected role of dispersing the active phase, may play a specific role in the catalyzed reaction itself, and in this regard, the so-called Strong metal-support interactions, existing between metals and semiconductor oxide supports such as titania and other oxides, are very well known (*1*).

In catalysts formed by metallic oxides supported on other metallic oxides, currently used to catalyze total or partial oxidation reactions, selection of a support is critical to increase the activity in one reaction or another. Thus, vanadia best oxidizes naphthalene (*2*) when supported on silica, on anatase is very effective at oxidizing *o*-xylene (*3*), and on alumina is especially active in benzene oxidation (*4, 5*); magnesium vanadates are very active catalysts for oxidative dehydrogenation of ethylbenzene to styrene (*6*). A similar behavior is observed with molybdena: reduction of NO with hydrogen is very effective when performed on MoO_3/ZrO_2, while reduction with ammonia is more effective when MoO_3/TiO_2 is used as catalyst (*7*).

In previous papers we have studied the incorporation of V_2O_5 on the surface of magnesia (*8*), silica, alumina, rutile (*9*), and anatase (*10*), and we have found that a relationship seems to exist between the basic–acidic character of the support and the way in which the supported phase interacts with it. Fransen *et al.* (*11*) have studied the properties of molybdena monolayer catalysts supported on several oxides, and they find the formation of bulk MoO_3 or a highly disperse phase, depending on the stoichiometry of the support. We have also studied (*8–10*) the effects of the use of several preparation methods on the properties of the catalysts obtained therefrom, as dispersion of the

[1] Present address: Escuela Universitaria Politécnica de Zamora, Spain.

[2] To whom correspondence should be addressed.

0021-9517/92 $3.00

supported phase and creation/removal of surface active sites markedly depends on the preparation method. Magnesium oxide is itself a catalyst for isomerization and exchange reactions, and its role as a support of active phases has been recently noted (*12*). In addition, the experimental conditions used to decompose $Mg(OH)_2$ to MgO and the effect of impurities on the surface properties, porosity, and crystallinity of MgO have also been studied (*13*).

In the present paper, MoO_3/MgO has been obtained from MgO prepared by dehydration of $Mg(OH)_2$ using two precursors of the supported phase: ammonium heptamolybdate (AHM), incorporated on the surface of magnesia by conventional impregnation from aqueous solutions, and MoO_3 itself, incorporated by manually grinding it as a mixture with MgO. For comparison purposes, some properties of the materials obtained when MoO_3 is incorporated on the surface of commercial MgO are also discussed (*14*).

EXPERIMENTAL

Materials. Commercial MgO (p.a) was from Panreac (Spain), ammonium heptamolybdate was from Carlo Erba, and MoO_3 was obtained from AHM after calcination in air at 770 K for 5 h. Chemical analyses for Mg and Mo in all samples studied were performed by atomic absorption in a Mark 2 ELL-240 instrument.

Sample preparation. Parent MgO was submitted to calcination overnight in air at 770 K to eliminate adsorbed organic impurities, leading to sample S. By mixing this oxide with MoO_3 and grinding manually in an agate mortar, sample M-S-0 was prepared, and from this, two samples, named M-S-1 and M-S-2, were obtained after calcining at 770 and 1100 K, respectively. These two samples are designated as "dry" samples.

In attempts to obtain similar samples by impregnation of MgO with aqueous solutions of AHM, a partial dissolution of the support is achieved, as previously observed when impregnating MgO with aqueous vanadate solutions (*8*), as the pH of the AHM solution is 2–2.5. In such a case, during heating to eliminate the solvent, $Mg(OH)_2$ precipitates and is then converted to MgO; so the changes observed in the texture properties of the solid, if compared to those of parent MgO, cannot be related to the presence of MoO_3. To avoid this, impregnation with AHM was carried out using solutions whose pH was previously adjusted to 11.9 with ammonia. The procedure was as follows. Support S was suspended in an aqueous ammonia solution at pH 11.9 and after being magnetically stirred for 2 h, the solvent was withdrawn in a rotary vacuum desiccator (Heidolph VV-60) at ≈320 K. According to its X-ray diffraction diagram, the solid thus obtained was $Mg(OH)_2$ (brucite). After calcination overnight at 770 K, the support named H was obtained, and MoO_3 was incorporated as described above for support S, leading to samples M-H-0 (uncalcined), M-H-1 (calcined at 770 K), and M-H-2 (calcined at 1100 K). A third series of samples was obtained by impregnating support H with an aqueous solution of AHM at pH 11.9 under experimental conditions as close as possible to those used to obtain this support, and then calcining at 770 or 1100 K, leading to samples I-H-0 (uncalcined), I-H-1 (calcined at 770 K) and I-H-2 (calcined at 1100 K). To compare the supported samples and the unloaded supports, oxides S and H were also submitted to calcination at 1100 K, leading to samples named S-2 and H-2, respectively. A summary of the preparation method is depicted in Fig. 1.

Calcination was performed at a heating rate of 10 K/min, using a quartz tubular furnace coupled to a temperature programmer–controller RAX P-C 8601 and maintaining the final temperature (770 or 1100 K) for 3 h. These two temperatures were chosen to yield decomposition of AHM and to melt MoO_3, respectively. Throughout the calcination process, a flow of 30 $cm^3\ min^{-1}$ of oxygen (from Sociedad Castellana del Oxígeno, S.C.O., Spain, 99.98%) was circulated over the samples.

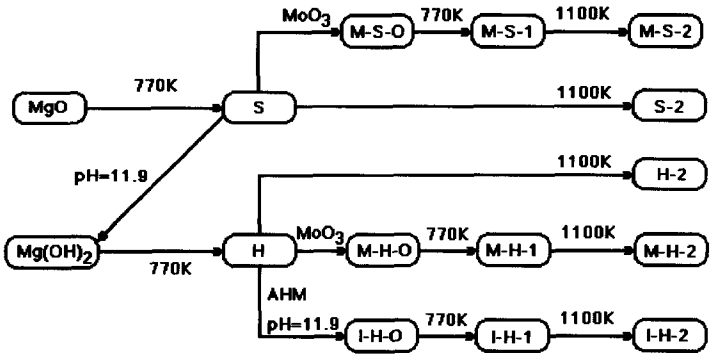

FIG. 1. Sample preparation.

The amounts of MgO and MoO_3 (or MgO and AHM) were chosen to yield final solids with a monolayer of MgO on MgO, as supported oxidation catalysts show optimum performances when the supported phase completely covers the surface of the support; in this way the active sites of the support become blocked, but the positive effect of the support on the active phase remains. Thus, according to the specific surface area of the supports (68.2 and 150.2 $m^2\ g^{-1}$ for supports S and H, respectively, see below) and taking the surface covered by a "molecule" of MoO_3 as 15×10^4 pm^2 (*11*), the compositions of the final solids obtained after calcination were 10.61 g MoO_3/100 g MgO on support S (atomic ratio Mo: Mg $\approx$ 1 : 34) and 23.94 g MoO_3/100 g MgO on support H (atomic ratio Mo : Mg $\approx$ 1 : 15).

Chemical analysis of all samples indicated that the thermal treatments given did not yield removal of molybdenum by sublimation as MoO_3.

Experimental methods. X-ray diffraction (XRD) diagrams were recorded in the range $3° \leq 2\theta \leq 60°$ in a Philips Model PW1030 diffractometer, using Ni-filtered Cu $K\alpha$ radiation (λ = 154.18 pm) and a goniometer speed of 1°(2θ)/min.

Differential thermal analysis (DTA) was performed in a Perkin–Elmer Model DTA-1700 apparatus, at a heating rate of 10 K min^{-1}, and flowing dry air (from S.C.O.) through the sample (50 $cm^3\ min^{-1}$). The instrument was coupled to a Perkin–Elmer 3600 data station.

UV–visible–NIR electronic spectra of the samples were recorded by diffuse reflectance in the wavelength range 850–200 nm using a Shimadzu UV-240 spectrophotometer coupled to a Shimadzu PR-1 graphic printer, parent MgO as a reference, and a spectral bandwidth of 5 nm; the spectra were submitted to a deconvolution analysis, assuming Gaussian-type curves and keeping the number of components to the minimum required to achieve a good fit.

Fourier transform infrared (FT–IR) spectra were recorded in a Perkin–Elmer FT-1730 instrument, coupled to a Perkin–Elmer 3700 data station. The KBr pellet technique was used, with a nominal resolution of 2 cm^{-1} and averaging 50 spectra.

Nitrogen adsorption isotherms were measured using nitrogen from S.C.O. in a conventional high-vacuum system (residual pressure 10^{-4} N m^{-2}), equipped with a silicone oil diffusion pump and grease-free taps; pressure changes were monitored with a MKS pressure transducer, and the system had been previously calibrated with helium (from S.C.O., 99.995%). Samples were outgassed *in situ* for 2 h at 420 K prior to adsorption experiments. Analyses of the isotherms for surface area and porosity measurements were performed with the assistance of a program run in an Apple Macintosh computer (*15*).

Temperature-programmed reduction (TPR) experiments were performed in a conventional system, with catharometric detection of hydrogen consumption, after condensing of water vapor with a dry ice/acetone cold trap. In all cases, samples containing ca. 20 μmol MoO_3 were used, with Ar containing 5% H_2 as carrier/reducer gas, and a heating rate of 10 K/min. These experimental conditions allow a precise resolution of the different steps of the reduction (*16*). No *in situ* treatment was performed.

Isoelectric point (IEP) measurements were performed in a Zeta-Meter Inc. Model ZM-77 instrument, provided with an automatic sample transfer system, using ca. 20 mg of sample in a solution of 200 cm^3 10^{-3} *M* KCl and adjusting the pH with 10^{-3} *M* solutions of KOH or HCl.

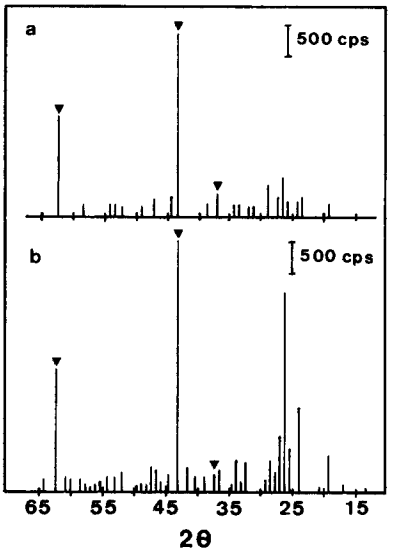

FIG. 2. X-ray diffraction diagrams of samples (a) I-H-2 and (b) M-H-2. Arrowed lines correspond to MgO.

RESULTS AND DISCUSSION

X-ray diffraction. All X-ray diffraction diagrams are dominated by the peak at 210.6 pm due to diffraction by the (200) planes of MgO; other peaks at 243 pm [(111) planes], and 149.1 pm [(220) planes] are also recorded. The peaks sharpen as the calcination temperature increases from support S to support S-2, suggesting a sintering at higher temperature. However, the peaks for support H are wider and weaker, indicating that calcination at 770 K after impregnation in aqueous ammonia has not been enough to achieve a good crystallization of the MgO crystallites formed upon dehydration of $Mg(OH)_2$.

Samples obtained by mechanical mixing and submitted to calcination at 770 K (M-S-1 and M-H-1) show, in addition to the MgO diffraction peaks, others originating from the presence of MoO_3. A very weak peak at 337 pm corresponding to diffraction by (220) planes of $MgMoO_4$ is also recorded for sample M-H-1. These results indicate that calcination at 770 K is able to yield reaction between the support and the supported phase, probably favored by the large specific surface area of the former (see below).

The XRD diagram for sample I-H-1 shows only wide, medium intense peaks of MgO, but no peak due to MoO_3, despite the fact that the calcination temperature (770 K) is high enough to decompose AHM to MoO_3. As both samples I-H-1 and M-H-1 had been obtained from the *same* support and contain the *same* amounts of Mo and Mg, it can be concluded that a good dispersion degree of the supported phase has been attained in sample I-H-1.

Independently of the way in which they have been obtained (impregnation or mechanical mixture) or the nature of the Mo precursor (molybdena or AHM), all samples calcined at 1100 K show fairly similar XRD diagrams. In addition to intense and sharp MgO peaks, all other peaks recorded originated only from $MgMoO_4$. As an example, the XRD diagrams corresponding to samples M-H-2 and I-H-2 are shown in Fig. 2. The differences observed should be due to a different degree of dispersion of $MgMoO_4$, as the chemical composition of both samples

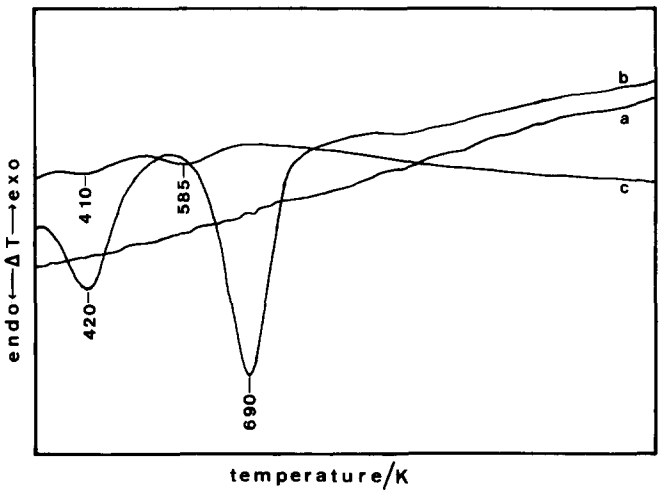

FIG. 3. Data profiles of precursors: (a) M-S-0; (b) I-H-0; and (c) M-H-0.

is the same. Molybdena should grow homogeneously on the surface of sample I-H-1 (from surface-attached molybdate precursors) and then reacts with the support leading to small crystallites of $MgMoO_4$ in sample I-H-2. On the contrary, molybdena crystallites in sample M-H-1 should be large (as this sample had been obtained by mechanical mixture) and then the $MgMoO_4$ crystallites formed therefrom upon calcination at 1100 K should also be fairly large, thus accounting for their intense XRD peaks in this sample.

Thermal analysis. No definite effects were recorded in the DTA profiles of the samples calcined at 770 or 1100 K, probably because the $MoO_3 \rightarrow MgMoO_4$ transformation is taking place over a wide temperature range and is not detected due to the low Mo loading. Two weak peaks are recorded at 820 and 910 K for a reference sample containing equimolecular amounts of MgO and MoO_3, the final product being $MgMoO_4$, as confirmed by its XRD diagram. According to a TG analysis of bulk AHM, decomposition to MoO_3 takes place at 570–670 K.

The DTA diagrams of the precursor samples are shown in Fig. 3. No peak is recorded above 770 K in any case. Two very small endothermic effects at 410 and 585 K are recorded for sample M-H-0, but no defined peak is observed in the diagram from sample M-S-0. As the supports in both samples had been calcined at 770 K before mixing with molybdena, the MgO crystallites should contain a very low surface concentration of water and hydroxyl groups. For sample I-H-0 two very intense endothermic effects are recorded, one at 420 K and another at 690 K, more intense and better defined. This last peak should be due to dehydroxylation of $Mg(OH)_2$ formed during impregnation, as the XRD diagram of sample I-H-0 shows only diffraction peaks of brucite, $Mg(OH)_2$; actually, the DTA diagram of $Mg(OH)_2$ obtained by impregnation of MgO with an ammonia solution at pH 11.9 shows only an intense endothermic effect at 680 K.

FT–IR spectroscopy. To assess if there is a reaction of molybdate species (in solution) with surface hydroxyl groups of MgO, the FT–IR spectra of the samples studied have been recorded. In no case were bands due to formation of carbonate species observed.

The FT–IR spectra of some of the samples in the 4000–3000 cm^{-1} range, where the bands due to $\nu_{O\text{-}H}$ modes are expected to be recorded, are shown in Fig. 4. For support

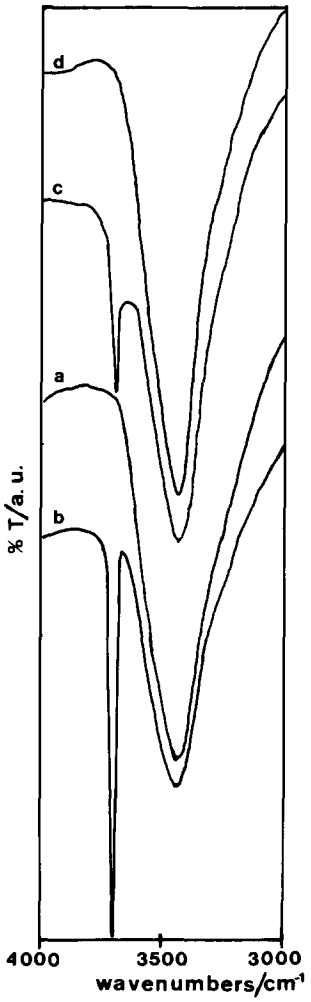

FIG. 4. FT-IR spectra of (a) support S; (b) support H before calcination at 770 K; (c) sample I-H-0; (d) sample I-H-1.

S only a wide band, centered at 3433 cm^{-1} and due to ν_{O-H} modes of hydrogen bonded hydroxyl groups, is recorded (Fig. 4a). A similar spectrum was recorded for support H submitted to calcination at 770 K. However, when the support is immersed in an aqueous solution of pH 11.9 and then dried at room temperature, the FT–IR spectrum (Fig. 4b) of the sample obtained (the XRD diagram of which indicates the exclusive presence of brucite, $Mg(OH)_2$) shows, in addition to this broad absorption, a sharp, very intense band at 3700 cm^{-1}, due to isolated surface hydroxyl groups. This same band is recorded, but with a much lower intensity, for precursor I-H-0 (Fig. 4c), and finally vanishes in the spectra of all samples calcined at 770 or 1100 K (the spectrum for sample I-H-1 is shown in Fig. 4d).

These results indicate that interaction of molybdate species with the surface of support H in aqueous solution at pH 11.9 (the same treatment given to sample responsible for spectrum 4b) takes place through surface, isolated hydroxyl groups of the support, in agreement with the previous results of Fransen *et al.* (*11*); the fact that a weak band is still recorded in the spectrum of sample I-H-0 indicates that a small number of hydroxyl groups still remain, unreacted, on the surface of this support.

Visible–ultraviolet spectra. The geometry of oxide ions surrounding Mo(VI) cations markedly affects the energy of charge transfer processes between both moieties, and so the presence of $[MoO_4]$ or $[MoO_6]$ species in our samples can be ascertained from their spectra, recorded by the diffuse-reflectance technique. For octahedral species two absorption bands should be recorded at 225 and 290–330 nm, while for $[MoO_4]$ species such bands are recorded at 225 and 260–280 nm (*17, 18*). Thus, the existence of bands above ca. 300 nm would account for the presence of $[MoO_6]$ species in our samples. However, recent results by Che and co-workers (*19, 20*) indicate that the position of these bands also depends (and even more markedly) upon other factors, such as size of the polyanion and nature of the countercation.

The electronic spectra of the precursor samples obtained by mechanical mixture (M-S-0 and M-H-0) show a wide band at 330–320 nm, due to $[MoO_6]$ species existing in MoO_3. Upon calcination at 770 K no change could be observed in the spectrum of sample M-S-1 (that is, octahedral species should remain unreacted), although for sample M-H-1 a good fit of the deconvoluted spectrum with the experimental one could

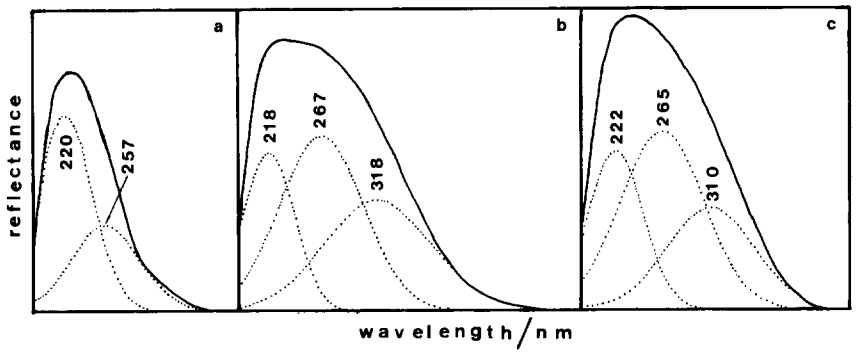

FIG. 5. Visible UV/DR spectra of samples (a) I-H-0; (b) I-H-1; and (c) I-H-2. Reference: MgO.

be achieved only by assuming a band at 250 nm in addition to that at 323 nm due to $[MoO_6]$ species. As XRD data (see above) indicated the presence of $MgMoO_4$ (which contains $[MoO_4]$ species), the band at 250 nm may be ascribed in this case to the presence of such tetrahedral moieties. This result indicates that in this sample part of the molybdena reacts with the support, leading to formation of $MgMoO_4$.

When calcination is performed at 1100 K, the absorption band at 310–325 nm vanishes, and both samples M-S-2 and M-H-2 show only two absorption bands at 220 and 270–280 nm, which, in agreement with the XRD patterns of these samples, should be ascribed to $[MoO_4]$ species ($MgMoO_4$).

On the other hand, samples belonging to series I show a very different behavior. The spectra are shown in Fig. 5. A wide band, with two components at 220 and 257 nm, is recorded for sample I-H-0. As $Mo_7O_{24}^{6-}$ species undergo a depolymerization process to $MoO_4^{=}$ species at pH above 10, it should be concluded that the band at 257 nm is due to the presence of $[MoO_4]$ species. Upon calcination at 770 K, a widening of the band takes place, with three components at 218, 267, and 318 nm, and thus the presence of $[MoO_4]$ and $[MoO_6]$ species can be tentatively concluded.

Calcination at 1100 K does not modify the spectrum much, although the absorption band widens and can be resolved now into three components at 222, 265, and 310 nm. These results indicate the probable presence of $[MoO_4]$ and $[MoO_6]$ species, although the XRD data indicated only the presence of the former as $MgMoO_4$.

Surface texture. Adsorption–desorption isotherms of nitrogen at 77 K on all samples were reversible in the relative pressure range studied ($0 \leq p/p_0 \leq 0.95$) and belonged to Type II in the IUPAC classification, with no hysteresis loop. Accordingly, micropores were absent and the specific surface area (SSA) values calculated following the BET, Cranston and Inkley, and t methods were coincident within experimental error. The values are collected in Table 1. Although these values seem to be erratic, a detailed study allows us to reach a series of interesting conclusions.

Figure 6 includes the change in the SSA values for the supports and the samples. For both supports, increasing the calcination temperature from 770 (S and H) to 1100 K (S-2 and H-2) leads to a decrease in the SSA. This decrease is larger in the case of support H than of support S, probably because this support, prepared from $Mg(OH)_2$, was not fully stabilized after calcination at 770 K. Such a decrease is also observed for samples containing molybdenum and calcined at 770 or 1100 K. Again, such a decrease is very much larger for samples prepared from support H than for that prepared with support S.

TABLE 1

Crystalline Phases (XRD, in Addition to MgO), Specific Surface Area (SSA, $m^2\ g^{-1}$), Isoelectric Point (IEP), and H_2 Consumption during TPR Runs (H_2/Mo) of the Supports and the Samples Studied

Sample	XRD	SSA	IEP	H_2/Mo
S	—	68	n.m.	0
S-2	—	48	11.7	0
M-S-1	MoO_3	66	10.4	3.0
M-S-2	$MgMoO_4$	56	10.7	3.4
H	—	150	n.m.	0
H-2	—	59	n.m.	0
M-H-1	MoO_3 + $MgMoO_4$[a]	123	11.0	1.9
M-H-2	$MgMoO_4$	77	9.4	1.8
I-H-1	—	270	11.2	2.0
I-H-2	$MgMoO_4$	83	11.5	1.6
MoO_3	MoO_3	nm[b]	6.3	3.1
$MgMoO_4$	$MgMoO_4$	nm	2.7	[c]

[a] Very weak.
[b] Not measured.
[c] See text.

If the values of samples containing molybdenum and calcined at 770 K are compared with those for the unloaded supports calcined at this same temperature, a decrease in the SSA is observed for samples prepared by mechanical grinding (series M-); but for the sample obtained by impregnation (I-H-1) a large increase is observed. The 80% increase in the SSA of sample I-H-1 with respect to that for support H can be ascribed to the fact that surface hydroxyl groups that should act as bridging sites between primary magnesia particles during sintering have been removed through reaction with $MoO_4^{=}$ species, as shown by the FT–IR spectra above. Such a decrease is almost negligible (only 3%) for sample M-S-1 if compared with support S, probably because the structure of this support is well stabilized and does not change by a further 2-h heating at 770 K.

However, the most interesting features come from samples containing molybdenum and calcined at 1100 K, when compared with the unloaded supports calcined at the same temperature. In these cases, an increase in SSA is always observed. In other words, the expected (and recorded) sintering of magnesia crystallites upon calcination at 1100 K is cancelled when molybdenum species are present. Molybdenum-containing species on the surface of magnesia in some

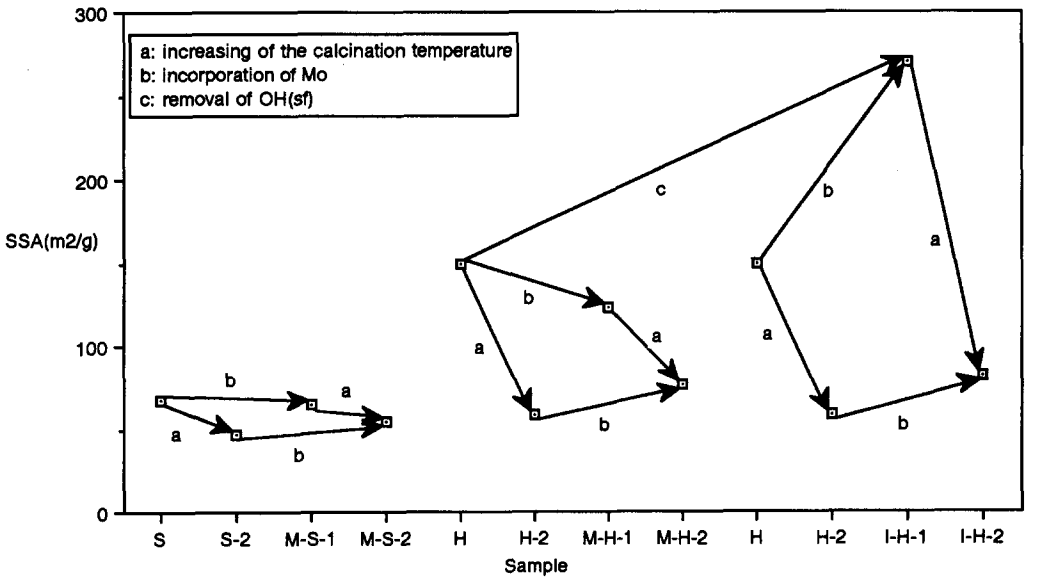

FIG. 6. Specific surface area of the supports and the samples and their change with thermal treatments and molybdenum incorporation.

way avoid a marked sintering of the particles.

These results are consistent with the fact that the specific gravity of $MgMoO_4$ (2.208 g cm^{-3}) is slightly larger than half of that of MgO (3.58 g cm^{-3}) and lower than half of that of MoO_3 (4.692 cm^{-3}), and so formation of the former during calcination at high temperature leading to a more opened structure should lead to an increase in the SSA.

Isoelectric point measurements. The results are summarized in Table 1. The values obtained for samples prepared from support S are fairly coincident (10.5 ± 0.2), indicating a decrease from the value obtained for unloaded magnesia (11.7). The values for MoO_3 and $MgMoO_4$ are much lower. The decrease in the IEP upon incorporation of MoO_3 indicates a partial covering of the surface of the support with molybdenum-containing species, although it cannot be ascertained which species, $MgMoO_4$ or MoO_3, exists, as the value determined for our samples, although lower than that for MgO, is higher than those for these species. This decrease is even more appreciable for sample M-H-2, with an IEP value of 9.4; however, for samples prepared by impregnation it is nearly the same as for unloaded MgO. In all cases, covering of the MgO surface by molybdenum-containing species is not complete, and the IEP values are not as low as those corresponding to MoO_3 and $MgMoO_4$. On the other hand, it is clear that both MoO_3 and $MgMoO_4$ should be simultaneously exposed on the MgO surface, and/or covering different percentages of surface in the different samples; if not, a steady decrease of the IEP values with the surface molybdenum content would be expected. However, plotting the IEP values vs the surface molybdenum concentration (as calculated from the Mo content and the actual specific surface area of the samples), as in Fig. 7, does not give rise to a steadily decreasing curve. The low IPE value found for sample M-H-2 can be related to the presence of large particles of $MgMoO_4$, as shown by the XRD results in Fig. 2.

Temperature-programmed reduction. The TPR profiles for all samples are shown in Fig. 8; the plots have been normalized to be referred to equivalent amounts of molybdenum in all of them.

Under the experimental conditions used here, the total reaction expected is

$$3\ H_2 + Mo^{VI} \rightarrow Mo$$

and then the expected consumption of hydrogen will be 3 mol H_2/mol Mo. The values indicated in Table 1 have been obtained upon integration of the area under the curve from 820 K (in the mechanical mixtures and bulk MoO_3) or from 670 K (in samples obtained by impregnation) up to 1170 K, assuming a linear, flat baseline and including the amount of hydrogen consumed during 15 min under an isothermal heating at 1170 K, the maximum temperature that could be reached under the experimental conditions used.

Although the TPR curves can be submitted to a deconvolution analysis similar to that used with the visible–UV spectra, this has not been performed, as such an analysis is extremely complicated because of melting of MoO_3 within the temperature range studied.

For bulk MoO_3 the main peak is recorded at 1020 K, with two other maxima at higher temperature, and total consumption of hydrogen is 3.1 H_2/Mo. The curves are nearly coincident for sample M-S-1 (3.0 H_2/Mo) and for sample M-H-1, although consumption in this case is only 1.9 H_2/Mo. The curve is ill-defined for sample M-S-2 and the consumption recorded, 3.4 H_2/Mo, is acceptable within experimental error. For sample M-H-2, again the curve is badly defined, but consumption is 1.8 H_2/Mo.

In samples obtained by mechanical mixture, MoO_3 existing after calcination at 770 K should be present as fairly large crystallites, with no interaction with the support, and its reduction profile and hydrogen consumption will be nearly coincident with those of bulk MoO_3.

Samples obtained by impregnation show

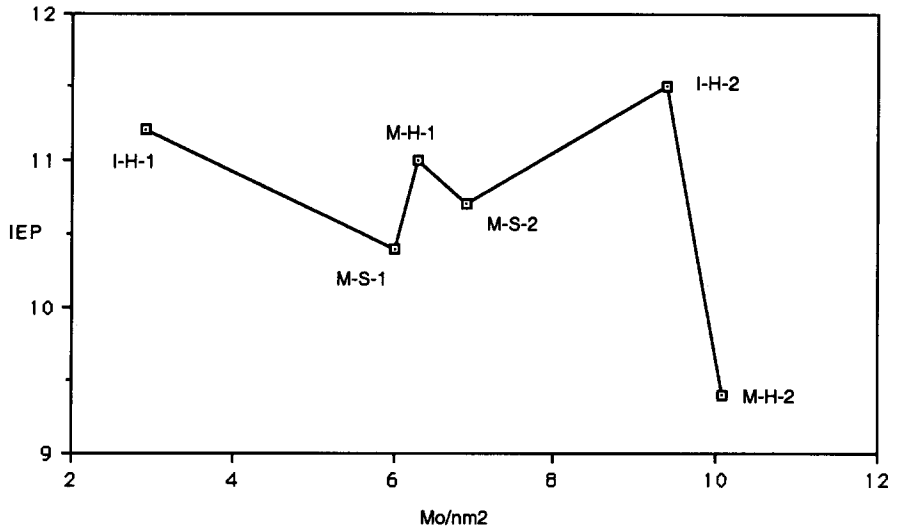

FIG. 7. Change in the IEP of the samples with the surface molybdenum content.

hydrogen consumptions well below the expected value (as samples M-H- do), but the shape of the TPR profiles is completely different, with a very well-defined maximum at 970–1000 K, and with a further hydrogen consumption at higher temperature, that has not been completed even at the maximum temperature reached. Hydrogen consumptions are similar to those of samples M-H-, 1.8 ± 0.2 H_2/Mo.

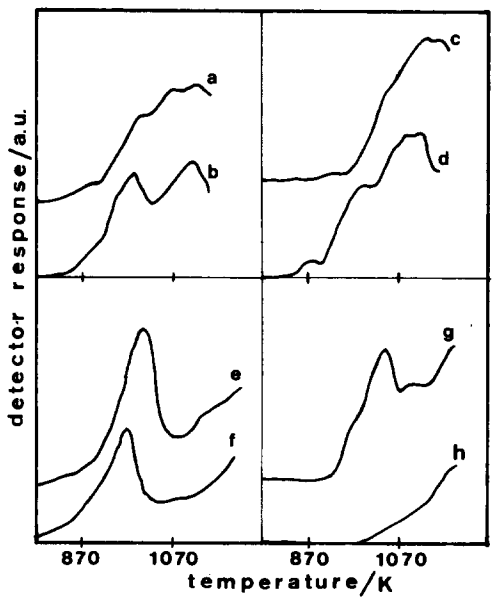

FIG. 8. TPR profiles of samples (a) M-S-1; (b) M-S-2; (c) M-H-1; (d) M-H-2; (e) I-H-1; (f) I-H-2; (g) MoO_3; and (h) $MgMoO_4$.

At first sight, it can be concluded that samples obtained by mechanical mixing show ill-defined curves, thus suggesting an analogy because of the preparation method, while samples obtained with support H show hydrogen consumptions ca. 40% lower than the expected ones, thus suggesting now an analogy because of the nature of the support.

It could alternatively be argued that a lower hydrogen consumption is due to a lower amount of molybdenum in the samples. However, this should be clearly discarded, as chemical analysis indicates that no MoO_3 sublimes by calcination at 770 or 1100 K.

The TPR profile of $MgMoO_4$ has also been recorded (Fig. 8) and shows that reduction of $MgMoO_4$ has barely started at the maximum temperature reached in our study. In other words, formation of molybdate renders difficult the reduction of molybdenum.

Brito and Lane (*21*) have studied the TPR of MoO_3 supported on alumina and silica

and have reported a dependence of the reduction profile on the nature of the support and the MoO_3 loading. These authors ascribe well-defined peaks to a good degree of crystallinity or homogeneity of the reducible species and establish a correlation between the strength of the MoO_3–support interaction and the reduction temperature of MoO_3 monolayers, this being higher as the former increases. With this, it can be assumed that the reduction profile of MoO_3 (and probably that of $MgMoO_4$) should be quite different when supported or when in a bulk state.

Samples prepared on support H show a completely different behavior. For samples belonging to series M-H- (with a larger SSA development than those belonging to series M-S-), calcination at 770 K leads to formation of small amounts of $MgMoO_4$ (XRD results above), probably in spots where MgO and MoO_3 crystallites are in contact. With that, during the reduction process, although the presence of $MgMoO_4$ in this sample and in that calcined at 1100 K leads to hydrogen consumptions lower than that corresponding to the stoichiometric reduction, the $MgMoO_4$ species should be present as fairly large particles, as suggested by two results: some of their XRD peaks are already detected after calcination at 770 K (contrary to sample I-H-1), and its XRD peaks are very intense (Fig. 2).

Finally, samples belonging to series I-H- show clean TPR profiles (Fig. 8), with only a well-defined maximum and an increase in the hydrogen consumption above the maximum temperature that can be experimentally reached. Molybdenum-containing species in sample I-H-1 should be very well dispersed, as none of their diffraction peaks are recorded. Calcination at 1100 K (sample I-H-2) leads to crystallization of $MgMoO_4$, but without increasing the crystallinity of the MoO_3 species, which should be present as a thin film on the MgO crystallites. As a result, the reduction profile, which should correspond to reduction of MoO_3, is almost identical in both cases, as the state of MoO_3 should also be very similar in both samples.

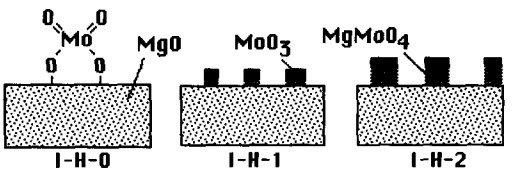

FIG. 9. Scheme depicting formation of MoO_3 and $MgMoO_4$ species on the surface of magnesia in samples obtained by impregnation.

On the contrary, reduction of $MgMoO_4$, better dispersed than in sample M-S-2 and M-H-2, will take place in a similar way in both cases.

CONCLUSIONS

From the results described above, it can be concluded that incorporation of MoO_3 on the surface of MgO leads to a weak interaction only when a high population of surface hydroxyl groups exists on the latter, such an interaction leading to $MgMoO_4$ formation. Incorporation from AHM solutions leads to highly dispersed MoO_3, stable even after calcining at 1100 K (treatment that, with the samples obtained by mechanical mixture, led to differently dispersed $MgMoO_4$). It can be concluded that in samples obtained by impregnation, the supported phase (MoO_3 and/or $MgMoO_4$) is forming two-dimensional structures, as depicted in Fig. 9. In sample I-H-0, discrete [MoO_4] species should exist on the MgO surface. Calcination at 770 K (sample I-H-1) leads to MoO_3 formation, and of $MgMoO_4$ in the magnesia–molybdena interface, but both $MgMoO_4$ and unreacted MoO_3 (located far away from the magnesia surface and its migration being unfavored because of the relatively low temperature) are highly dispersed, decorating the MgO particles as a film that does not completely cover the magnesia surface (according to the IEP results). Calcination at 1100 K to yield sample I-H-2 makes easy the sintering of the different species, thus giving rise to a sharpening and intensification of their XRD peaks, as well as to a decrease of the SSA. Although sintering of MoO_3 crys-

tallites would also be expected, the fact that calcination is carried out at a temperature high enough to melt it, leads to its redispersion, the MoO_3 particles thus being undetectable by XRD.

ACKNOWLEDGMENTS

Financial support from CICYT (project MAT88-0556) and Consejería de Cultura y Bienestar Social de la Junta de Castilla y León is greatly appreciated.

REFERENCES

1. Tauster, S. J., *Acc. Chem. Res.* **20,** 389 (1987).
2. Westerman, D. W. B., Foster, N. R., and Wainwright, M. S., *Appl. Catal.* **3,** 141 (1982).
3. Wachs, I. E., Saleh, R. Y., Chan, S. S., and Chersich, C. C., *Appl. Catal.* **15,** 339 (1985).
4. Lucas, J., Van Der Well, D., and Waugh, K. C., *J. Chem. Soc. Faraday Trans. 1* **77,** 15 (1981).
5. Lucas, J., Van Der Well, D., and Waugh, K. C., *J. Chem. Soc. Faraday Trans. 1* **77,** 31 (1981).
6. Hanuza, J., Jezowska-Trzebiatowska, B., and Oganowski, W., *J. Mol. Catal.* **29,** 109 (1985).
7. Hattori, H., Tanabe, K., Tanaka, K.-I., and Okazaki, S., *in* "Chemistry and Uses of Molybdenum, Third International Conference" (H. F. Barry and P. C. H. Mitchell, Eds.), pp. 188–193. Climax Molybdenum Co., 1979.
8. Del Arco, M., Holgado, M. J., Martín, C., and Rives, V., *J. Mater. Sci. Lett.* **6,** 616 (1987).
9. Del Arco, M., Holgado, M. J., Martín, C., and Rives, V., *Langmuir* **6,** 801 (1990).
10. Del Arco, M., Holgado, M. J., Martín, C., and Rives, V., *J. Catal.* **99,** 19 (1986).
11. Fransen, T., van Berge, P. C., and Mars, P., *in* "Preparation of Catalysts" (B. Delmon, P. A. Jacobs, and G. Poncelet, Eds.), pp. 405–416. Amsterdam, Elsevier, 1976.
12. Guglielminotti, E., *Langmuir* **2,** 812 (1986).
13. Wanke, S. E., and Fiedorov, R. M. J., *in* "Characterization of Porous Solids" (K. K. Unger, J. Rouquerol, and K. S. W. Sing, Eds.), pp. 601–609. Amsterdam, Elsevier, 1988.
14. Llorente, J. M. M., and Rives, V., *Solid State Ionics* **38,** 119 (1990).
15. Martin, C., Rives, V., and Malet, M., *Powder Technol.* **46,** 1 (1986).
16. Malet, P., and Caballero, A., *J. Chem. Soc. Faraday Trans. 1* **84,** 2369 (1988).
17. Ashley, J. H., and Mitchell, P. C. H., *J. Chem. Soc. A* 2821 (1968).
18. Giordano, N., Bart, J. C. H., Vaghi, A., Castellan, A., and Martinotti, G., *J. Catal.* **36,** 81 (1975).
19. Fournier, M., Louis, C., Che, M., Chaquin, P., and Masure, D., *J. Catal.* **119,** 400 (1989).
20. Masure, D., Chaquin, P., Louis, C., Che, M., and Fournier, M., *J. Catal.* **119,** 415 (1989).
21. Brito, J., and Laine, J., *Polyhedron* **5,** 179 (1986).